Molecular Biology of the Cell
Vol. 20, 2049–2059, April 1, 2009

Diacylglycerol Kinase ζ Regulates Actin Cytoskeleton Reorganization through Dissociation of Rac1 from RhoGDI

Hanan Abramovici,[*†] Parmiss Mojtabaie,[*†] Robin J. Parks,[†‡§] Xiao-Ping Zhong,[‖] Gary A. Koretzky,[¶] Matthew K. Topham,[#] and Stephen H. Gee[*†]

[*]Department of Cellular and Molecular Medicine, University of Ottawa, Ottawa, Ontario K1H 8M5, Canada; [‡]Molecular Medicine Program, Ottawa Health Research Institute, Ottawa, Ontario K1H 8L6, Canada; [†]Centre for Neuromuscular Disease, University of Ottawa, Ottawa, Ontario, Canada; [§]Department of Biochemistry, Microbiology and Immunology, University of Ottawa, Ottawa, Ontario, Canada; [#]Huntsman Cancer Institute and Department of Internal Medicine, University of Utah, Salt Lake City, UT 84112; [‖]Departments of Pediatrics and Immunology, Duke University Medical Center, Durham, NC 27710; and [¶]The Signal Transduction Program, Abramson Family Cancer Research Institute, Philadelphia, PA 19104

Submitted December 14, 2007; Revised January 30, 2009; Accepted February 3, 2009
Monitoring Editor: Martin A. Schwartz

Activation of Rac1 GTPase signaling is stimulated by phosphorylation and release of RhoGDI by the effector p21-activated kinase 1 (PAK1), but it is unclear what initiates this potential feed-forward mechanism for regulation of Rac activity. Phosphatidic acid (PA), which is produced from the lipid second messenger diacylglycerol (DAG) by the action of DAG kinases (DGKs), is known to activate PAK1. Here, we investigated whether PA produced by DGKζ initiates RhoGDI release and Rac1 activation. In DGKζ-deficient fibroblasts PAK1 phosphorylation and Rac1–RhoGDI dissociation were attenuated, leading to reduced Rac1 activation after platelet-derived growth factor stimulation. The cells were defective in Rac1-regulated behaviors, including lamellipodia formation, membrane ruffling, migration, and spreading. Wild-type DGKζ, but not a kinase-dead mutant, or addition of exogenous PA rescued Rac activation. DGKζ stably associated with PAK1 and RhoGDI, suggesting these proteins form a complex that functions as a Rac1-selective RhoGDI dissociation factor. These results define a pathway that links diacylglycerol, DGKζ, and PA to the activation of Rac1: the PA generated by DGKζ activates PAK1, which dissociates RhoGDI from Rac1 leading to changes in actin dynamics that facilitate the changes necessary for cell motility.

INTRODUCTION

Rho GTPases regulate gene transcription, cell cycle progression, vesicular traffic, and cell polarity (Jaffe and Hall, 2005; Ridley, 2006) but are best known for their ability to coordinate alterations in cellular actin networks that regulate cell morphology. Such changes are necessary for directed cell migration during embryogenesis, inflammation, wound healing, and tumor metastasis (Burridge and Wennerberg, 2004). In mammalian cells, Rac1 promotes actin polymerization and focal complex assembly, leading to lamellipodia protrusion and membrane ruffle formation; Cdc42 regulates filopodial extension; and Rho promotes the assembly of actin stress fibers and focal adhesions (Ridley *et al*., 1992; Nobes and Hall, 1995).

This article was published online ahead of print in *MBC in Press* (http://www.molbiolcell.org/cgi/doi/10.1091/mbc.E07–12–1248) on February 11, 2009.

Address correspondence to: Stephen H. Gee (stevegee@uottawa.ca).

Abbreviations used: BSA, bovine serum albumin; DAG, diacylglycerol; DGK, diacylglycerol kinase; DMEM, Dulbecco's modified Eagle's medium; FCS, fetal calf serum; GFP, green fluorescent protein; GST, glutathione transferase; HA, hemagglutinin; HRP, horseradish peroxidase; PA, phosphatidic acid; PAK1, p21-activated kinase 1; PBD, p21-binding domain; PDGF, platelet-derived growth factor; YFP, yellow fluorescent protein.

All Rho GTPases cycle between inactive GDP-bound and active GTP-bound conformations; the active versions interact with specific downstream effectors to elicit distinct biological responses. This cycle is tightly regulated by guanine nucleotide exchange factors (GEFs), which activate GTPases by promoting the exchange of guanosine diphosphate (GDP) for guanosine triphosphate (GTP), and by GTPase-activating proteins (GAPs), which inactivate Rho proteins by enhancing their intrinsic GTPase activity. A third class of proteins, guanine nucleotide dissociation inhibitors (GDIs), regulates Rho GTPase function in as many as three distinct ways. RhoGDI, the best characterized member, 1) prevents GDP dissociation, 2) inhibits intrinsic or GAP-stimulated GTP hydrolysis (Chuang *et al*., 1993b), and 3) regulates GTPase partitioning between the cytosol and plasma membrane (Olofsson, 1999). The latter task is accomplished by sequestering the GTPases as soluble cytosolic complexes in which the C-terminal membrane-targeting lipid moiety is prevented from interacting with membranes (Dermardirossian and Bokoch, 2005; Dovas and Couchman, 2005). Dissociation of GTPases from RhoGDI is a prerequisite for membrane association and activation by GEFs. Because the majority of Rho GTPase protein exists in a biologically inactive cytosolic complex with RhoGDI in resting cells, this a major point of regulation of Rho GTPase activity and function (Chuang *et al*., 1993a; Olofsson, 1999).

The selective activation of individual Rho GTPases by growth and/or adhesive factors implies that separate mech-

anisms must exist to dissociate them from cytosolic RhoGDI complexes and target them to the appropriate membrane domain. The means by which Rho family proteins are released from RhoGDI is poorly understood, and so far no common mechanistic theme has emerged. Dissociation seems to use several different mechanisms, including direct phosphorylation by protein kinases (Bourmeyster *et al*., 1992; Mehta *et al*., 2001; Dermardirossian *et al*., 2004) and protein displacement factors such as integrins, ERM proteins, and the p75 NGF receptor (Takahashi *et al*., 1997; Del Pozo *et al*., 2002; Yamashita and Tohyama, 2003).

Accumulating evidence suggests negatively charged phospholipids play an important role in RhoGDI release (Bourmeyster *et al*., 1992; Chuang *et al*., 1993a; Faure *et al*., 1999; Dovas and Couchman, 2005; Ugolev *et al*., 2006). Among those shown to dissociate RhoGDI, phosphatidic acid (PA) is particularly interesting because it also activates p21-activated kinase 1 (PAK1) (Bokoch *et al*., 1998), a downstream effector of activated Rac and Cdc42 implicated in the regulation of multiple cellular activities, including cytoskeletal dynamics (Bokoch, 2003). Recently, PAK1 was shown to bind to and phosphorylate RhoGDI, resulting in the selective release of Rac1 (Dermardirossian *et al*., 2004). Thus, PA-mediated activation of PAK1 might initiate Rac signaling, but precisely how this occurs and the source of PA are unclear.

Diacylglycerol kinases (DGKs) phosphorylate the lipid second messenger diacylglycerol (DAG) to yield PA and are thus a potential source for PA-mediated Rac activation. Supporting this possibility, Tolias *et al*. (1998) found that Rac/RhoGDI exists in a complex with a DGK, and we recently demonstrated that the ubiquitously expressed ζ isoform binds directly to Rac1 (Yakubchyk *et al*., 2005). Here, we investigated the possibility that DGKζ might be part of a Rac/PAK1 complex and a source of PA for PAK1 activation by analyzing the phenotype and biochemical properties of embryonic fibroblasts from DGKζ-null mice. Our findings demonstrate that DGKζ is part of a signaling complex that functions as a Rac1-selective RhoGDI dissociation factor and define a direct link between lipid second messengers and regulation of the actin cytoskeleton.

MATERIALS AND METHODS

Antibodies

Monoclonal hemagglutinin (HA), actin, tubulin, and α-actinin antibodies were from Sigma-Aldrich (St. Louis, MO). Monoclonal Rac1 and paxillin antibodies were from BD Biosciences (San Jose, CA). Monoclonal RhoA and polyclonal RhoGDI were from Santa Cruz Biotechnology (Santa Cruz, CA). Polyclonal PAK1 was from Cell Signaling Technology (Danvers, MA). Anti-pPAK1 was a gift from Dr. Jonathan Chernoff (Fox Chase Cancer Center, Philadelphia, PA). The DGKι antibody was a gift from Dr. Kaoru Goto (Yamagata University School of Medicine, Yamagata, Japan). Polyclonal Phospho-Akt Ser473 and Akt were from Cell Signaling Technology. Monoclonal phospho-tyrosine (clone 4G10) was from Millipore Bioscience Research Reagents (Temecula, CA). A polyclonal antibody raised against the N terminus of DGKζ is as described previously (Topham *et al*., 1998). Monoclonal antibody 1351 was a gift from Dr. Stanley Froehner (University of Washington, Seattle, WA). AlexaFluor 488- and 594-conjugated secondary antibodies and phalloidin were from Invitrogen (Carlsbad, CA). Horseradish peroxidase-conjugated anti-rabbit and anti-mouse secondary antibodies were from Jackson ImmunoResearch Laboratories, Inc. (West Grove, PA).

Reagents

Matrigel was from BD Biosciences. FuGENE 6 transfection reagent was from Roche Diagnostics (Indianapolis, IN). DMEM was from Invitrogen. Protein A agarose was from Millipore Bioscience Research Reagents. 1,2-dioctanoyl-*sn*-glycero-3-phosphate (08:0 PA), 1,2-dioctanoyl-*sn*-glycerol (08:0 DAG), and 1-hexanoyl-2-hydroxy-*sn*-glycero-3-phosphate (06:0 LPA) were from Avanti Polar Lipids (Alabaster, AL). All other reagents were from Sigma-Aldrich.

Plasmids and Constructs

Plasmids encoding wild-type DGKζ and a kinase-dead mutant (DGK$\zeta^{\Delta ATP}$), both with three tandem, N-terminal HA epitope tags, as well as DGKζ with a C-terminal FLAG epitope tag (DGKζ^{FLAG}), have been described previously (Topham *et al*., 1998; Hogan *et al*., 2001). The PAK1-p21-binding domain (PBD) and Rhotekin-RBD constructs were as described previously (Sander *et al*., 1998; Ren *et al*., 1999). N-terminal myc-tagged Rac1^{V12} in pEFmPLINK was a gift from Dr. Andrew Thorburn (University of Colorado, Denver, CO). N-terminal yellow fluorescent protein (YFP)-tagged Rac1^{V12} was generated by subcloning Rac1^{V12} from pEFmPLINK into the KpnI and ApaI sites of pEYFP-C1 (Clontech, Mountain View, CA). The full-length GST-RhoGDI construct was generated by subcloning mouse RhoGDI from pcDNA 3.1 (UMR cDNA Resource Center; www.cdna.org) into the EcoRI and XhoI cloning sites of pGEX-4T-1.

Cell Culture and Transfection/Infection

Primary mouse embryonic fibroblasts (MEFs) were isolated from wild-type (+/+) and DGKζ-deficient (−/−) embryos (13.5 d after coitus) as described previously (Robertson, 1987). MEFs were cultured in DMEM supplemented with 10% fetal calf serum (FCS), 2 mM L-glutamine, 100 U ml^{-1} penicillin, and 100 U ml^{-1} streptomycin and grown at 37°C, 5% CO_2. Immortalized cell lines were generated by transfecting MEFs with pcDNA3.1 harboring a simian virus 40 large T antigen expression cassette and the *Sh ble* antibiotic resistance gene. Stable clones were selected in media containing 200 μg ml^{-1} Zeocin (Invitrogen).

For Rac1^{V12} experiments, cells were transfected with either myc- or YFP-tagged Rac1^{V12} constructs for 24 h. Cells were fixed in 4% paraformaldehyde (PFA) and then processed for immunocytochemistry (for myc-Rac1^{V12}) or live microscopy (for YFP-Rac1^{V12}).

Cloning and production of adenoviral constructs encoding green fluorescent protein (GFP), wild-type (wt) DGKζ, DGKζ^{FLAG}, or the kinase-dead mutant have been described previously (Yakubchyk *et al*., 2005). For rescue experiments, fibroblasts were infected with adenoviruses at a multiplicity of infection of 100–250 (for ruffling rescue and Rac1 activity assays) or 1000 (for wounding assays) for 1 h at 37°C. Cells were further incubated for 24–36 h under standard growth conditions.

Immunofluorescence Microscopy and Quantification of Actin-based Structures

Fibroblasts were seeded onto Matrigel-coated coverslips, serum starved overnight, and then stimulated with either platelet-derived growth factor (PDGF)-BB (Sigma-Aldrich) or vehicle (0.14M HCl and 0.1% bovine serum albumin [BSA]). Cells were fixed and processed as described previously (Abramovici and Gee, 2007). Images were obtained using a charge-coupled device (CCD) camera on an Axioskop 2 microscope (Carl Zeiss, Jena, Germany). To quantify actin-based structures, fixed cells were labeled with AlexaFluor 488- or 594-conjugated phalloidin. A lamellipodium was an area of the cell with thick peripheral F-actin within a broad, sheet-like region; a peripheral ruffle was a curvilinear accumulation of F-actin at the cell edge; circular ruffles were circular accumulations of F-actin on the dorsal cell surface, and filopodia finger-like, actin-rich protrusions. A minimum of 200 cells were counted for each phenotype. For rescue experiments, all cells were assumed to have been infected. Cell and ruffle surface areas were measured using the "outline" tool function in AxioVision 4.5 software (Carl Zeiss).

Adhesion Assays

Adhesion assays were performed as described previously (Wagner *et al*., 2002). Cells were plated at a density of 2×10^4/coverslip for the indicated times and processed for immunofluorescence microscopy as described above.

Wounding Assays

Cell monolayers on 12-mm coverslips were scraped with a 20-gauge needle, generating wounds ~0.2 × 12 mm. Three wounds were made on each coverslip. Cells were fixed with 0.5% PFA immediately (0 h) or after 2 h incubation at 37°C. Cells were stained with AlexaFluor-conjugated phalloidin (or indicated antibodies) and prepared for immunofluorescence microscopy. Photomicrographs were taken at 500-μm intervals along the length of the wound, images were exported into AxioVision 4.5 software, and the extent of cell migration was quantified by two independent methods, both yielding similar results. The wound width was determined by lines drawn perpendicular to the wound edge at 50-μm intervals. The percentage wound closure was calculated by subtracting wound width at 2 h from 0 h and dividing the resulting number by wound width at 0 h. In the second method, the area devoid of cells was manually traced with the outline tool function and the wound area automatically calculated by the software. Measurements at 2 h were then subtracted from the wound area at 0 h and divided by wound area at 0 h. Data were exported into Excel (Microsoft, Redmond, WA), and then graphed using SigmaPlot software (SPSS, Chicago, IL).

Transwell Migration Assays

Modified Boyden chamber assays were performed as described previously (Sander *et al*., 1998). Fibronectin (FN)-coated filters were placed into the lower chamber containing either 0.1% BSA or 50 ng ml^{-1} PDGF-BB. Wild-type or DGKζ-null MEFs (1×10^5) resuspended in 0.1% BSA in DMEM were added to the upper chamber and allowed to migrate for up to 12 h. Cells were fixed with 4% PFA for 30 min and stained with 4,6-diamidino-2-phenylindole. Ten randomly selected fields were photographed and counted for each experiment.

Immunoprecipitation and Glutathione Transferase (GST) Pull-Down Experiments

Immunoprecipitations were carried out essentially as described previously (Hogan *et al*., 2001). To measure Rac1-RhoGDI dissociation, wt and DGKζ-null MEFs were serum-starved overnight and then stimulated with 50 ng ml^{-1} PDGF for 5 min. Cells were lysed in lysis buffer (50 mM Tris-HCl, pH 7.5, 50 mM NaCl, 5 mM $MgCl_2$, 1% NP-40, 5% glycerol, 1 mM dithiothreitol (DTT), and protease inhibitors and centrifuged at 18,000 × *g* for 10 min at 4°C. Equivalent amounts of protein (~1 mg) were incubated with 5 μg RhoGDI antibody or control rabbit immunoglobulin G (IgG) for 4 h at 4°C. Then, 40 μl of 50% protein G agarose slurry was added for 1.5 h. The beads were washed with lysis buffer, resuspended in 1× reducing sample buffer, and analyzed for bound RhoGDI or Rac1 by immunoblotting. GST pull-down experiments were carried out as described previously (Yakubchyk *et al*., 2005) by using lysis buffer without $MgCl_2$. For some experiments, wt fibroblasts were infected with HA-DGKζ, and the cells were harvested 24 h later.

Rho GTPase Activity Assays

Levels of active Rac1 and Cdc42 were measured using a GST-PAK1 PBD pull-down assay (Sander *et al*., 1998). Cells were serum starved overnight and then stimulated with 50 ng ml^{-1} PDGF for 3 min for Rac1 assays or with 100 ng ml^{-1} bradykinin for 4 min for Cdc42 assays. For lipid assays, serum-starved cells were treated with 100 nM PA, DAG, LPA, or vehicle for 25 min at 37°C. After stimulation, media were removed, and cells were immediately harvested in chilled lysis buffer (50 mM Tris-HCl, pH 7.4, 150 mM NaCl, 1% Triton X-100, 20 mM $MgCl_2$, and protease inhibitors). Lysates were incubated for 10 min at 4°C and then centrifuged at 18,000 × *g* for 10 min. Equivalent amounts of protein were incubated with GST-PAK1 PBD beads for 30 min at 4°C. The beads were washed with lysis buffer, boiled in reducing sample buffer, and eluted proteins assayed for bound Rac1 or Cdc42 by immunoblotting. For PAK1 inhibition experiments, cells were incubated with dimethyl sulfoxide or 30 μM of the PAK1 inhibitor IPA-3 (Deacon *et al*., 2008) for 20 min at 37°C before stimulation with 25 ng/μl^{-1} PDGF for 5 min.

Quantification of Phosphorylated PAK1

Fibroblasts were seeded onto 100-mm dishes and grown until confluent. Cells were treated as indicated and then lysed directly in reducing sample buffer. Lysates were boiled, sonicated, and analyzed by immunoblotting using an affinity-purified phospho-specific PAK1 antibody (Sells *et al*., 2000) or a polyclonal anti-PAK1 antibody. Digital images were captured using a Kodak Image Station 440 CF (Eastman Kodak, Rochester, NY), and band intensity was measured by densitometric analysis. To calculate relative amounts of pPAK1, the intensity of the upper band of the pPAK doublet was normalized to total PAK and expressed as a percentage of the unstimulated, wt condition.

Live-Cell Imaging

Imaging was carried out using an Axiovert 200 M microscope (Carl Zeiss) with a stage-fixed cell chamber at 37°C, 5% CO_2. Equal numbers of wild-type or DGKζ-null fibroblasts were cultured in 35-mm dishes (MatTek, Ashland, MA) and were serum-starved overnight and then stimulated with 50 ng ml^{-1} PDGF for 15 min. For ruffling experiments, cells were imaged at a 100× magnification by using a differential interference contrast III filter, and filmed at 10-s intervals for 15 min by using an Axiocam HRm charge-coupled device (CCD) camera.

Small Interfering RNA (siRNA) Experiments

Two siRNA oligonucleotides (oligo) corresponding to nucleotides 1679-1701 and 2480-2502 of human DGKζ and control scrambled versions were used: oligo 1 sense, ACA GCC GCU UUC GGA AUA AdTdT and antisense, UUA UUC CGA AAG CGG CUG UdTdT; oligo 2 sense, UCG CAC AGG AUG GA UUU AdTdT and antisense, UAA AUC UCA UCC UGU GCG AdTdT; scrambled oligo 1 sense, GGU CAU UCC AAC GAC AGU AdTdT and ant-sense, UAC UGU CGU UGG AAU GACCdTdT; and scrambled oligo 2 (sense), GGA AAG UAU CGC GUU CUA AdTdT and antisense, UUA GAAC GCG AUA CUU UCC dTdT.

HeLa cells were grown to ~80% confluence in growth medium (DMEM supplemented with 10% FCS, 2 mM L-glutamine, and 100 U ml^{-1} penicillin/streptomycin), washed twice with phosphate-buffered saline, and then transferred to DMEM. siRNA oligos were diluted in Opti-MEM (Invitrogen) to a final concentration of 200 nM and mixed with Oligofectamine (Invitrogen). After 4 h of transfection, the medium was replaced with DMEM supplemented with 5% FCS. The cells were returned to growth medium the next day and then harvested 24–48 h later.

Two-Dimensional (2D) Gel Electrophoresis

Cells were harvested in chilled lysis buffer (50 mM Tris-HCl, pH 7.6, 150 mM NaCl, 1% Triton X-100, 1 mM DTT, 1 mM activated sodium orthovanadate, 10 mM sodium fluoride, 2 mM sodium pyrophosphate, and 2 mM β-glycerophosphate). Lysates were centrifuged at 10,000 × *g* for 10 min at 4°C. The supernatants were centrifuged at 100,000 × *g* for 1 h at 4°C. 100 μg of the final supernatants were precipitated with 4 volumes of acetone overnight at −20°C. The precipitates were pelleted at 13,000 × *g* at 4°C for 10 min, air-dried, and then resuspended in urea/thiourea rehydration solution (7 M urea, 2 M thiourea, 2% 3-[(3-cholamidopropyl)dimethylammonio]propanesulfonate, 0.5% IPG buffer, pH 3–11 NL, 1% DTT, and 0.0005% bromophenol blue). The protein solution was loaded into reswelling trays, and IPG strips (pH 3–10) were applied to the trays. Isoelectric focusing was carried out as follows: 300 V for 4 h, 1000 V for 30 min, 5000 V for 1.5 h, 5000 V for 30 min, and 500 V for 20 h. IPG strips were incubated 10 min each in equilibration buffer (6 M urea, 75 mM Tris-HCl, pH 8.8, 29.3% glycerol, 2% SDS, and 65 mM DTT) and then in equilibration buffer lacking DTT but containing 135 mM iodoacetamide. Strips were then transferred to SDS-polyacrylamide gels for second dimension electrophoresis.

RESULTS

Generation of DGKζ-deficient Mouse Embryonic Fibroblasts

To investigate potential roles for DGKζ in Rac1-regulated events, we established immortalized fibroblast cell lines derived from wild-type mice or mice in which the DGKζ gene was disrupted by homologous recombination (Zhong *et al*., 2003). DGKζ-deficient MEFs did not express detectable levels of the DGKζ protein (Supplemental Figure S1A). To determine whether the loss of DGKζ leads to compensatory up-regulation of other DGKζ family members, extracts of wt and null MEFs were immunoblotted with an antibody to DGKι, the most closely related isoform. No differences in total DGKι levels were observed (Supplemental Figure S1B), suggesting fibroblasts do not compensate for the lack of DGKζ by modulating the expression of DGKι. The levels of several other relevant proteins remained unchanged in the DGKζ-null cells (Supplemental Figure S1C).

Decreased Rac1 Activation in the Absence of DGKζ

To determine whether the absence of DGKζ affects Rac1 activation, the level of GTP-bound (active) Rac1 was assayed in lysates of wt and null cells by using an effector pull-down assay (Sander *et al*., 1998). There was no significant difference in resting Rac1-GTP levels between serum-starved wt and null cell lysates (Figure 1A; data not shown). There was a substantial increase in Rac1-GTP levels in wt cell lysates after PDGF stimulation as expected, but only a small increase in null cell lysates (Figure 1, A and B). Thus, these data reveal a dramatic decrease in PDGF-dependent Rac1 activation in the absence of DGKζ. There was no appreciable difference in Cdc42 activity between the wt and null lysates, either with or without bradykinin stimulation (Figure 1C). Independent verification of the above-mentioned results was obtained by siRNA knockdown of DGKζ in HeLa cells. An oligonucleotide targeted to DGKζ caused a marked reduction in DGKζ protein levels and a parallel decrease in active Rac, whereas a scrambled version had no discernible effect (Figure 1D). To demonstrate that the change in Rac activity is due directly to the loss of DGKζ, the wt protein was reintroduced into null cells by adenoviral infection (Figure 1E). Protein expression was verified by immunoblotting cell lysates with an anti-DGKζ antibody. PDGF-stimu-

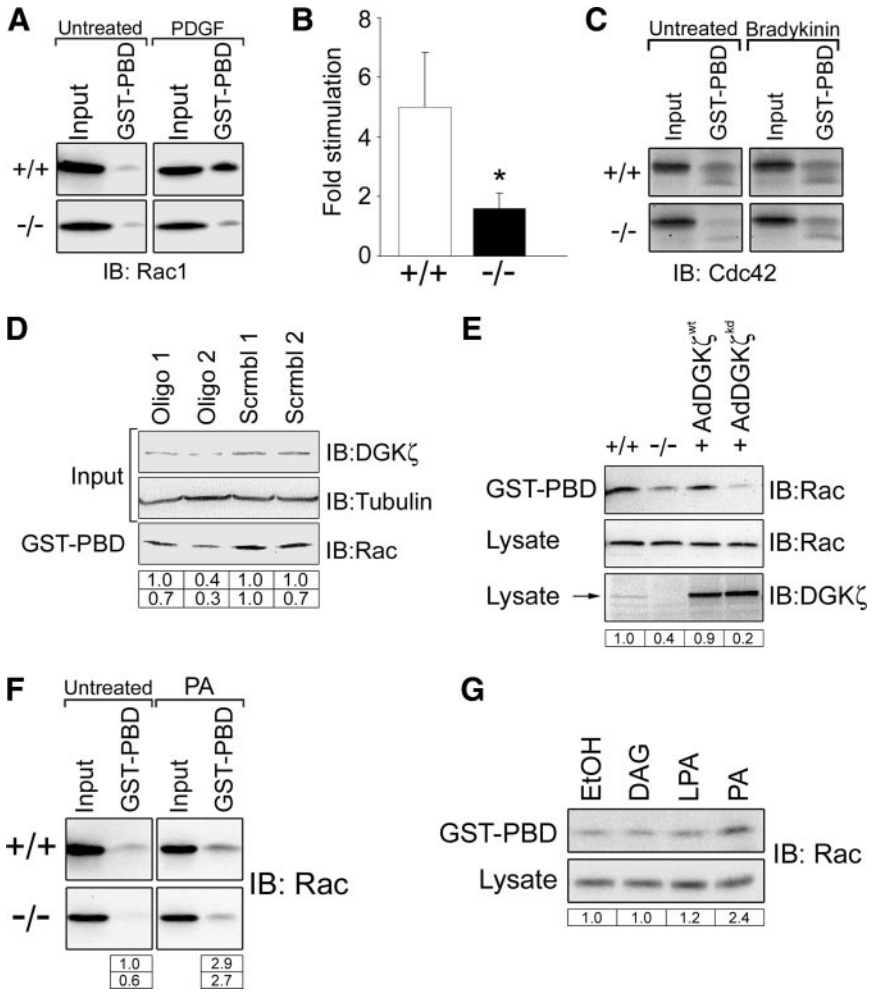

Figure 1. Decreased Rac1 activation in DGKζ-null fibroblasts following PDGF stimulation. (A) Assay of global Rac1 GTPase activity. Serum-starved wt (+/+) and DGKζ-null (−/−) fibroblasts were treated 5 min with PDGF or vehicle alone (untreated). Cell lysates were incubated with immobilized GST-PBD, and the bound proteins were analyzed by immunoblotting (IB) for Rac1. Input represents ~5% of the starting material. (B) Quantification of active Rac levels by densitometric analysis of immunoblots. Values are the -fold change ± SEM in active Rac after PDGF stimulation from three independent experiments. The asterisk indicates a statistically significant difference from wt ($p < 0.001$) by Student's *t* test. (C) Cdc42 activity was assayed as described in A by using fibroblasts treated 5 min with bradykinin or vehicle. (D) siRNA-mediated knockdown of DGKζ. HeLa cells were treated with the indicated siRNAs as described in *Materials and Methods*. The lysates were immunoblotted for DGKζ and tubulin or assayed for Rac activity as described in A. The tabulated values indicate relative levels of DGKζ (top row) and of active Rac (bottom row) normalized to tubulin levels. (E) Rescue of Rac activation requires DGKζ catalytic activity. DGKζ-null cells were infected with adenovirus bearing HA-tagged wt or kinase-dead (kd) DGKζ. Rac activity, and total Rac content was assayed as described above in PDGF-stimulated wt, DGKζ-null, and infected null cell lysates. The levels of endogenous and HA-tagged DGKζ (arrow) were detected with an anti-DGKζ antibody. (F) Serum-starved wt and DGKζ-null cells were treated for 25 min with 100 μM PA, and then Rac activity was determined as described above. (G) Serum-starved DGKζ-null cells were treated for 25 min with vehicle (ethanol [EtOH]) or with 100 μM DAG, LPA, or PA, and then Rac activity was assayed as described above. The tabulated values in D, E, and F indicate the relative amount of active Rac1 in each sample normalized to total Rac1 and to active Rac1 in wt cells.

lated Rac1 activity in lysates of cells expressing wt DGKζ (AdDGKζ^{wt}) was noticeably increased compared with uninfected control cell lysates. In contrast, a kinase-dead mutant (AdDGKζ^{kd}) failed to increase active Rac levels. These results strongly suggest the Rac activation defect in null cells is due to the loss of DGKζ activity.

To determine whether the defect is due to decreased PA production by DGKζ and hence could be rescued by exogenous PA, wt and null cells were treated with a membrane-permeable form of PA, and the lysates were subsequently analyzed for Rac activity (Figure 1F). Exogenous PA increased Rac activity in both wt and null cell lysates to a similar extent (~3–4-fold). In control experiments, neither DAG nor LPA caused a detectable increase in Rac activity in DGKζ-null cells (Figure 1G). Collectively, these results suggest DGKζ-derived PA contributes to the regulation of Rac activity after PDGF stimulation.

Decreased PAK1 phosphorylation in DGKζ-Null Cells

The PAKs are Ser/Thr protein kinases whose activity is regulated by binding of active Rac or Cdc42. Because Rac1 activity was decreased in DGKζ-null cells, we investigated whether there was a corresponding decrease in active PAK1. Binding of active Rac or Cdc42 to PAK1 relieves autoinhibition and stimulates autophosphorylation, leading to increased kinase activity (Bokoch, 2003). Thus, the level of pPAK, as determined by immunoblotting with a phospho-specific antibody, was used to gauge PAK activity. In unstimulated wt cells, two pPAK1 bands were evident (Figure 2A); the upper band most likely represents hyperphosphorylated PAK1 and the lower band, a less phosphorylated version (Sells *et al*., 2000). There was a substantial decrease in the levels of both bands in DGKζ-null cells. When normalized to total PAK1 levels, the intensity of the upper pPAK1 band was only about half that seen in wt cells (Figure 2B).

We next assayed pPAK levels in cells stimulated by PDGF, which is known to activate PAK1 (Dharmawardhane *et al*., 1997). A previous report noted only a slight increase (28%) in total pPAK1 levels upon PDGF stimulation by measuring the fluorescence intensity of individual, immunolabeled fibroblasts (Sells *et al*., 2000). Consistent with this, we found global pPAK levels in PDGF-treated wt cells were not significantly different from unstimulated cells (Figure 2B), despite the same concentration of PDGF being able to induce substantial membrane ruffling (data not shown). It is likely that small differences in individual cells do not translate into a biochemically detectable difference among a large population. Nevertheless, as for unstimulated cells, PDGF-stimulated null cells had only half as much pPAK1 as wt cells (Figure 2B).

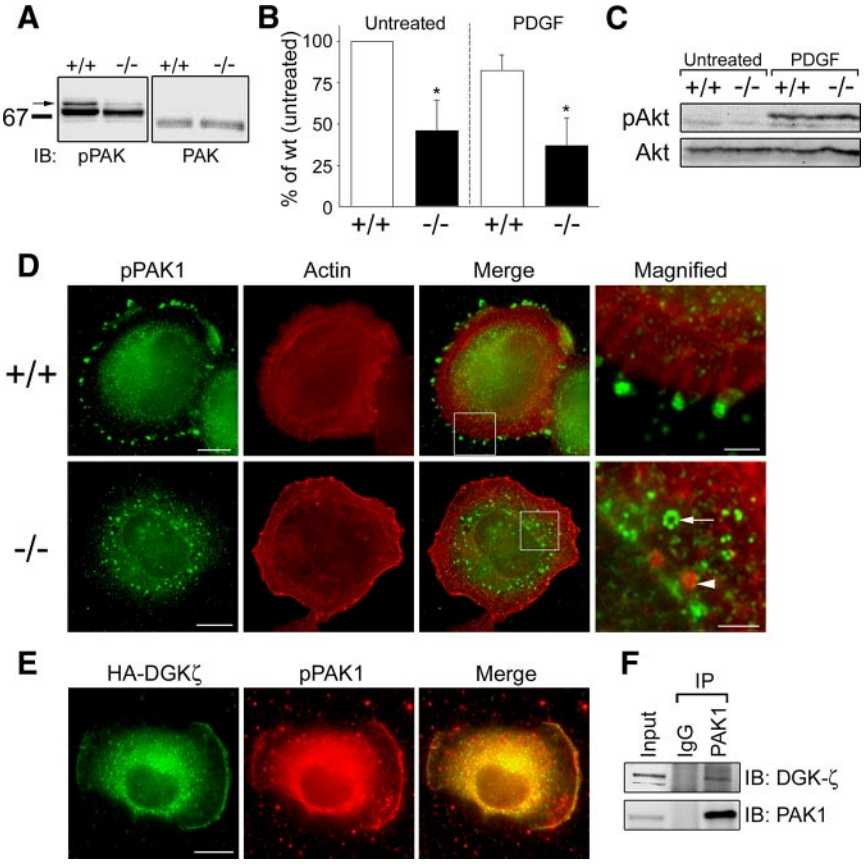

Figure 2. Decreased PAK1 phosphorylation in DGKζ-null fibroblasts. (A) Detergent extracts prepared from serum-starved wt and DGKζ-null cells were analyzed by immunoblotting for phosphorylated (p)PAK1 and total PAK1. (B) Quantification of pPAK1 levels by densitometric analysis of immunoblots. The top pPAK1 band (arrow in A) was measured and normalized to total PAK levels. Values are means ± SD from six independent experiments. Asterisks denote a significant difference from untreated wt cells ($p < 0.05$) by Student's *t* test. (C) PDGF-induced Akt phosphorylation is unaffected by loss of DGKζ as assessed by immunoblotting wt and null cell extracts with a pAkt antibody. (D) Mislocalization of pPAK1 in DGKζ-null fibroblasts. Cells seeded onto fibronectin-coated coverslips were fixed 45 min after plating then double labeled with an anti-pPAK1 antibody (green) followed by AlexaFluor 488-conjugated secondary antibody and with AlexaFluor 594-conjugated phalloidin (red). Bar, 10 um. (E) Colocalization of DGKζ and pPAK1 at lamellipodia edges. Fibroblasts transfected with HA-tagged DGKζ were fixed 30 min after replating and then stained with anti-HA and anti-pPAK antibodies. Bar, 10 um. (F) Interaction of endogenous DGKζ and PAK1. Detergent extracts of wt fibroblasts were incubated with normal rabbit IgG or an antibody to PAK1. Immune complexes were precipitated with protein G agarose then analyzed by immunoblotting with anti-PAK1 and anti-DGKζ antibodies. Input represents 3% of starting material.

Extracellular stimuli can activate PAK1 via multiple independent pathways (Bokoch, 2003; Menard and Mattingly, 2003). Akt, a serine/threonine kinase that is rapidly phosphorylated after growth factor stimulation, phosphorylates PAK1 via a GTPase-independent mechanism (Welch *et al*., 1998; Tang *et al*., 2000). Therefore, we assessed whether the Akt pathway is altered in DGKζ-null cells by immunoblotting with an anti-pAkt antibody. The loss of DGKζ had no detectable effect on pAkt levels after PDGF stimulation (Figure 2C), suggesting signaling upstream of Akt is not impaired in DGKζ-deficient fibroblasts.

PAK1 Localization

In resting cells, PAK1 is localized to membranous structures within the cytoplasm (Dharmawardhane *et al*., 1997). However, active PAK1 preferentially accumulates in dynamic actin-based structures such as focal adhesions and membrane ruffles (Dharmawardhane *et al*., 1997; Sells *et al*., 1997, 2000), most likely via its association with one or more binding partners (Bokoch *et al*., 1996; Manser *et al*., 1998; Bagrodia *et al*., 1999; Manabe *et al*., 2002). To determine whether DGKζ influences the targeting of active PAK1 to adhesive sites, wt and DGKζ-null cells were stained for pPAK1 after replating cells for 45 min on fibronectin. As expected, pPAK1 labeling in wt cells was concentrated in focal adhesions (identified by their typical radiating actin bundles) on the cell's circumference (Figure 2D). In contrast, pPAK1 was confined to a perinuclear, cytoplasmic compartment in DGKζ-null cells. At higher magnification, pPAK1 foci in the null cells seem to be organized into circular profiles, suggesting they are associated with cytoplasmic vesicles. The localization of total PAK1 was mainly cytoplasmic and not obviously different in wt and null cells (Supplemental Figure S2A). We verified that focal adhesions are formed normally in DGKζ-null cells by using phosphotyrosine immunoreactivity as an indicator of focal adhesion formation (Supplemental Figure S3A). In wt cells, DGKζ was not concentrated in the majority of focal adhesions, revealed by staining for phosphorylated FAK (FAK-pY861; Supplemental Figure S3B). It was, however, codistributed with diffuse FAK-pY861 in areas rich in focal adhesions (Supplemental Figure S3C). Presumably, these are areas in which focal adhesions are in dynamic flux. Collectively, these data suggest DGKζ is required for the correct targeting of pPAK1 to focal adhesions but that it does not recruit pPAK to these sites.

In support of an interaction between DGKζ and pPAK, we found that HA-DGKζ colocalized with pPAK at the edge of lamellipodia in fibroblasts that were transfected with HA-DGKζ for 24 h and then replated for 30 min on FN (Figure 2E). DGKζ also specifically coimmunoprecipitated with PAK1 from extracts of wt fibroblasts (Figure 2F), suggesting the two proteins form a stable complex in cells.

Decreased RhoGDI Phosphorylation and Rac1 Release in DGKζ-Null Cells

After PDGF stimulation, PAK1 phosphorylates RhoGDI at two sites to initiate Rac release and activation (Dermardirossian *et al*., 2004). Because active PAK1 is decreased in DGKζ-null cells, we investigated whether there was a parallel reduction in RhoGDI phosphorylation by using 2D gel electrophoresis and immunoblotting. Stimulation of wild-type cells with PDGF induced the appearance of a more acidic RhoGDI spot, consistent with the addition of phosphate groups (Figure 3A, arrow). This spot, which seems identical

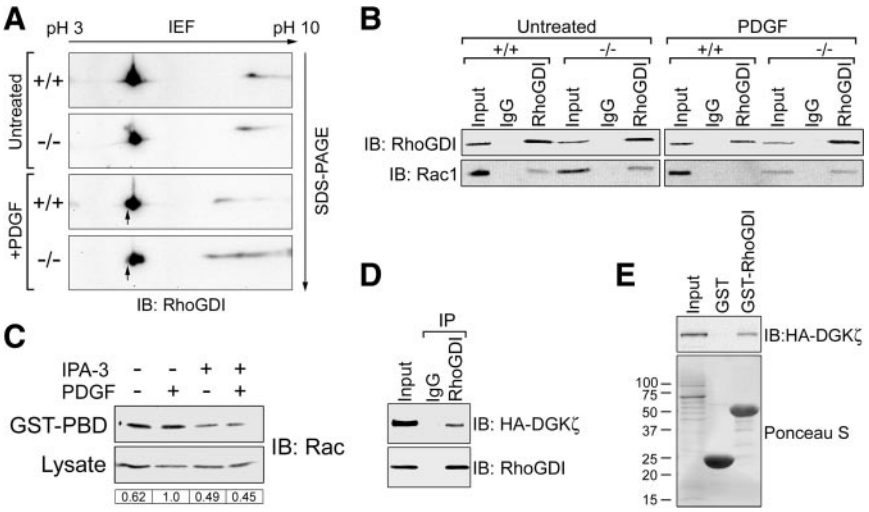

Figure 3. DGKζ is required for PDGF-induced dissociation of Rac1 from RhoGDI. (A) Serum-starved wt (+/+) and DGKζ-null (−/−) cells treated 5 min with PDGF or vehicle (untreated) were lysed and then analyzed by 2D gel electrophoresis and immunoblotting (IB) for RhoGDI. The arrow indicates a more acidic form induced after PDGF stimulation of wt, but not null cells. Data are representative of two independent experiments. (B) Cells treated as described in A were harvested and RhoGDI immunoprecipitated from the detergent-solubilized particulate fraction. Immune complexes were analyzed by immunoblotting for RhoGDI and Rac1. Data are representative of three independent experiments. (C) Serum-starved wt cells treated 5 min with PDGF or vehicle were incubated with or without 30 μM of the PAK1 inhibitor IPA-3. Rac activity was assayed by incubating the lysates with immobilized GST-PBD and analyzing the bound proteins by immunoblotting. The tabulated values indicate the relative amount of active Rac1 in each sample normalized to total Rac1. (D) Detergent extracts of wt cells infected with adenovirus bearing HA-tagged, wt DGKζ were incubated with control rabbit IgG or RhoGDI antibody. Immune complexes were analyzed by immunoblotting with anti-HA and anti-RhoGDI antibodies. (E) Lysates prepared as described in D were incubated with immobilized GST or GST-RhoGDI. The amount of each fusion protein is shown in the Ponceau S-stained blot. Bound proteins were analyzed by immunoblotting with an anti-HA antibody. In each case, input represents ~5% of the extract.

to the spot observed by Dermardirossian *et al*. (2004) after expression of constitutively active PAK1, was greatly reduced in intensity in DGKζ-null cells. These data suggest there is a defect in RhoGDI phosphorylation in DGKζ-null cells in response to PDGF stimulation.

Next, we assessed whether Rac1 release from RhoGDI is attenuated after PDGF stimulation. The amount of Rac1 bound to RhoGDI was assayed by coimmunoprecipitation from lysates of unstimulated and PDGF-stimulated wt and DGKζ-null cells (Figure 3B). Rac1 coprecipitated with RhoGDI from lysates of unstimulated but not stimulated wt cells, suggesting PDGF induces the dissociation of Rac from RhoGDI under these conditions. The amount of Rac1 that coimmunoprecipitated with RhoGDI from unstimulated null cell lysates was comparable to wt; however, PDGF stimulation did not decrease it, suggesting a defect in the release of Rac from RhoGDI in the absence of DGKζ.

Consistent with the idea that PAK1 acts upstream of RhoGDI and Rac1, treatment of wild type cells with a highly selective, small-molecule PAK1 inhibitor (Deacon *et al*., 2008) decreased both the steady state and the PDGF-stimulated increase in active Rac levels (Figure 3C).

We assessed potential interactions between DGKζ and RhoGDI by immunoprecipitating the latter from lysates of wt fibroblasts expressing HA-tagged DGKζ and immunoblotting the bound proteins. HA-DGKζ was coprecipitated by anti-RhoGDI but not by control IgG (Figure 3D). In addition, a GST-RhoGDI fusion protein, but not GST alone, captured HA-DGKζ from fibroblast extracts (Figure 3E). Together, these results suggest DGKζ and RhoGDI form a stable complex in cells.

DGKζ-Null Fibroblasts Have Fewer Lamellipodia and Membrane Ruffles

Rac1 regulates the formation of lamellipodia and membrane ruffles, structures that are driven by dynamic and spatially regulated changes in the actin cytoskeleton at the leading edge of migrating cells (Ridley *et al*., 1992). Two types of ruffles can generally be distinguished in cells stimulated by growth factors: peripheral ruffles, which are associated with active lamellipodia; and dorsal, circular ruffles (Abercrombie *et al*., 1970). DGKζ is concentrated in peripheral ruffles, at the leading edge of lamellipodia (Topham and Prescott, 2001; Abramovici *et al*., 2003; Luo *et al*., 2004a) and in circular ruffles, along with syntrophin and Rac1 (Supplemental Figure S4). To determine whether the defect in Rac activation affects lamellipodia and/or membrane ruffle production, these structures were quantified in fixed wt and null cells. Lamellipodia were observed in 67 ± 7% of wt fibroblasts grown in serum-containing media but in only in 24 ± 2% of null cells grown under identical conditions (Figure 4A). A similar deficiency in lamellipodia formation was noted after PDGF stimulation of serum-starved cells (data not shown). Similarly, PDGF-induced peripheral ruffling was significantly reduced in DGKζ-null cells (Figure 4B). Finally, there was an approximately threefold decrease in the frequency of PDGF-induced circular ruffles in null cells (Figure 4C). Circular ruffling in DGKζ-null cells was rescued by HA-tagged wt DGKζ but not by a kinase-dead mutant (Figure 4D), demonstrating that enzymatic activity is required. Together, these data indicate the formation of lamellipodia and ruffles is impaired by the loss of DGKζ.

To examine the possibility that ruffle formation is delayed rather than deficient, we compared living wt and null cells using time-lapse digital microscopy. We limited our study to circular ruffles because they are readily imaged using differential interference microscopy and follow a stereotypical time course (Buccione *et al*., 2004). After ~2-min PDGF stimulation, virtually every wt cell initiated a transient wave of circular ruffling that began at the cell periphery and progressed inwards (Supplemental Video 1). The majority of wt cells had completed ruffling 10 min after the onset of stimulation. In contrast, circular ruffling was severely impaired in DGKζ-null cells (Supplemental Video 2). Only a few null cells formed ruffles and in those that did, the ruffles were delayed by 1–2 min and were usually smaller and much less conspicuous. No additional circular ruffling was initiated for the duration of the recording (15 min). Thus, video imaging reveals a profound defect in circular ruffling in DGKζ-null cells.

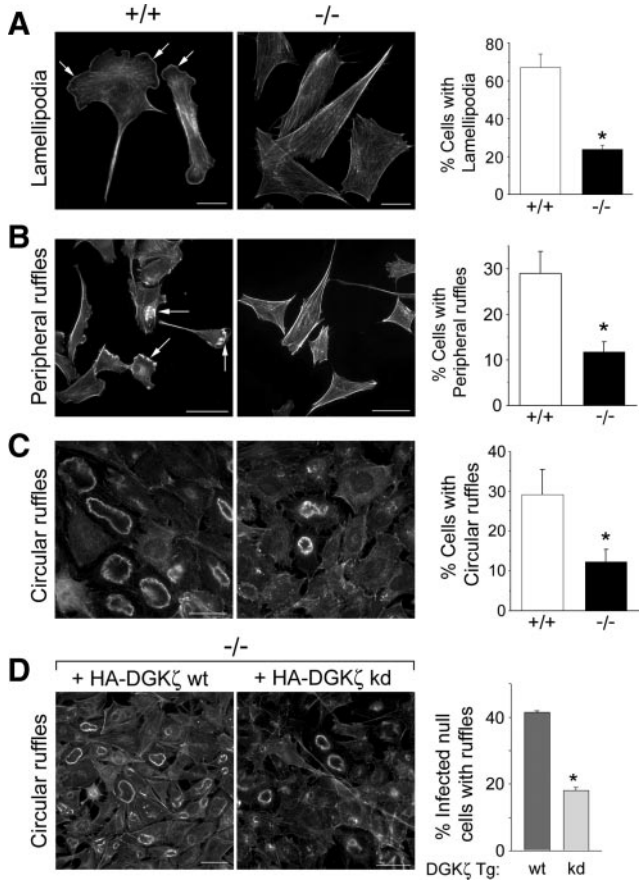

Figure 4. Impaired ruffling and lamellipodia formation in DGKζ-null fibroblasts. Representative images of wt (+/+) and DGKζ-null (−/−) fibroblasts stained with AlexaFluor 488-conjugated phalloidin showing lamellipodia (A, arrows), peripheral membrane ruffles (B, arrows), and circular ruffles (C). The cells shown in A were grown in media containing 10% serum, whereas cells in B and C were serum-starved overnight and then stimulated with 10 ng/ml PDGF for 5 min. Bars, 20 μm. The graph to the right of each pair of images shows the quantification of each structure in wt and null cells. In each case, values are the mean ± SEM from at least three independent experiments. A minimum of 200 cells were counted per condition. The asterisks denote a significant difference between wt and null cells ($p < 0.05$) by Student's *t* test. (D) Reintroduction of wt DGKζ rescues circular ruffling. Representative images of DGKζ-null cells infected with adenoviruses bearing HA-tagged versions of wt DGKζ (HA-DGKζ wt) or a kinase-dead mutant (HA-DGKζ kd). Bars, 50 μm. The graph shows the quantification of circular ruffling in infected null cells fixed and stained to reveal actin. Values are the mean ± SEM from two independent experiments. The asterisk denotes a significant difference ($p < 0.005$) by Student's *t* test. More than 200 cells were counted per condition.

Impaired Lamellipodia Formation in DGKζ-Null Cells

Given the failure of DGKζ-null cells to assemble PAK1 at focal adhesions, we evaluated the extent of integrin-mediated cell spreading and the morphology of the spreading cells by immunofluorescence microscopy at various times after replating on fibronectin. Wild-type cells stained for actin were generally cuboid and had numerous membrane ruffles (Figure 5A). After 60 min, they had fewer ruffles and were generally well spread. In contrast, null cells were stellate and had numerous large filopodia and substantially fewer membrane ruffles. However, the extent of spreading at 60 min was not significantly different. Quantitative analysis revealed a substantial reduction in membrane ruffling in the null cells 15 and 30 min after replating and a proportional increase in filopodia. Thus, DGKζ-null cells seem to have a defect in lamellipodial formation but normal filopodial extension.

Migration Is Impaired in DGKζ-deficient Fibroblasts

Wounding of a confluent cell monolayer induces lamellipodia formation and membrane ruffling at the leading edge; this requires Rac1 and Cdc42 activity (Nobes and Hall, 1999). We therefore assessed the ability of wt and DGKζ-null MEFs to undergo coordinated cell migration in a wound closure assay (Nobes and Hall, 1999; Fenteany *et al*., 2000). DGKζ-null cells exhibited a marked reduction in wound closure compared with wt cells when assayed 2 h after wounding (Figure 6, A and B). By 4 h after wounding, however, both wt and null MEFs had closed the wound, indicating that migration is not completely blocked in the null cells (data not shown). These data suggest DGKζ-null MEFs migrate less than their wt counterparts.

To determine whether the loss of DGKζ was the primary cause of the reduced migration, the wt protein was reintroduced into null MEFs. We verified that exogenously expressed DGKζ was properly localized in the null fibroblasts. In wt fibroblasts, endogenous DGKζ colocalized with Rac1 in lamellipodia along the edge of cells facing the wound (Figure 6C), consistent with previous reports (Abramovici *et al*., 2003; Luo *et al*., 2004a). Similarly, HA-DGKζ was concentrated at the leading edge of null MEFs migrating into the wound, where it colocalized with actin (Figure 6C). These data suggest exogenous DGKζ is correctly targeted to the front of migrating cells. Consistent with this finding, HA-DGKζ restored the migration of null MEFs to near wt levels, whereas expression of GFP in the null MEFs did not significantly increase wound closure (Figure 6, D and E). Collectively, these data suggest the migration defect of the null MEFs is directly attributable to the loss of DGKζ and that proteins required for normal DGKζ localization are largely unaltered.

Three-dimensional migration was assessed using modified Boyden chamber assays. The number of DGKζ-null MEFs that randomly migrated through a porous membrane (haptotaxis) was not significantly different from wt MEFs after 4 h (Figure 6F). However, in response to a PDGF gradient, significantly fewer null cells migrated across the membrane (chemotaxis), suggesting directional migration is impaired.

DISCUSSION

The interaction of Rho family proteins with RhoGDI is a major point of regulation of GTPase activity. Because they share a common inhibitor, different mechanisms should exist to specifically dissociate Rho GTPases from RhoGDI. However, the signaling mechanisms responsible are poorly understood (Dermardirossian *et al*., 2004; Dovas and Couchman, 2005). Our results suggest DGKζ is part of a signaling complex that functions as a Rac1-selective RhoGDI dissociation factor.

The finding that the basal Rac1-GTP level was unaffected in DGKζ-null cells but that the PDGF-stimulated level was substantially decreased compared with wt cells indicates a defect in Rac1 activation. Consistent with such a defect, the phenotype of the cells is remarkably similar to that of Rac1-null MEFs including; altered morphology, defects in lamellipodia formation and membrane ruffling, and a marked reduction in PAK phosphorylation (Nobes and Hall, 1999;

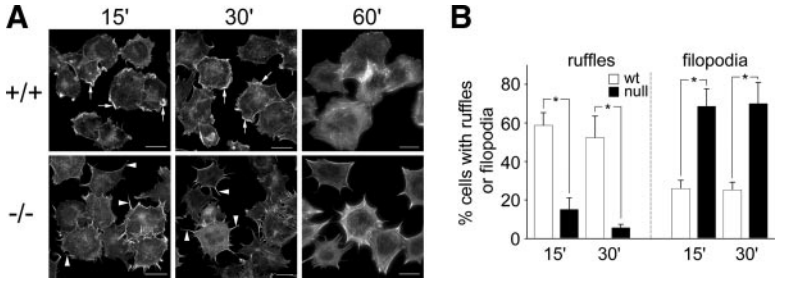

Figure 5. The absence of DGKζ affects cell spreading on fibronectin. Wt (+/+) and DGKζ-null (−/−) cells were plated on fibronectin-coated coverslips, incubated at 37°C for the indicated times, and then fixed and stained with AlexaFluor 594-conjugated phalloidin. (A) Typical morphology of wt and null cells after replating. Arrows indicate membrane ruffles, and arrowheads indicate the filopodia. Bars, 20 μm. (B) Random fields (n = 10) of wt and null cells were scored for the presence of ruffles and filopodia. A minimum of 100 cells was counted per condition. Data are displayed as the percentage (mean ± SEM) of total cells per field. Asterisks indicate a significant difference from wt ($p < 0.05$) by Student's *t* test.

Guo *et al*., 2006; Vidali *et al*., 2006). In contrast, Cdc42 activity did not seem to be impaired in the absence of DGKζ. Supporting this conclusion, DGKζ-null cells replated on FN contained numerous filopodia, which are regulated by integrin-induced activation of Cdc42 (Price *et al*., 1998).

The finding that Rac and RhoGDI associate with enzymes regulating phosphoinositide metabolism, including DGK and phosphoinositide kinase 5, lead to the suggestion of a lipid kinase signaling complex that regulates Rac activation (Tolias *et al*., 1998, 2000). Our data showing DGKζ binds directly to Rac1 (Yakubchyk *et al*., 2005) and associates in a complex with RhoGDI and PAK1 supports the idea that Rac1 resides in a regulated signaling complex whose function is to control the selective activation of Rac1 and the regulation of actin cytoskeletal dynamics. Moreover, because DGKζ also associates with phospholipase C (PLC) γ1 (Luo *et al*., 2004b), which hydrolyzes phosphatidylinositol 4,5-bisphosphate to yield DAG and inositol triphosphate, it seems to occupy a central position in an inositol lipid signaling pathway leading to Rac activation.

Phosphatidic Acid and Rac Activity

The role phosphoinositides play in Rac activity is complex; they act both upstream and downstream of Rac to drive actin reorganization in response to extracellular signals (Burridge and Wennerberg, 2004). The available evidence suggests PA and other anionic phospholipids lie upstream of Rac activation. PA dissociates Rac1-RhoGDI complexes (Bourmeyster *et al*., 1992; Chuang *et al*., 1993a; Mesmin *et al*., 2004; Tolias *et al*., 1998; Ugolev *et al*., 2006) and activates PAK1 (Bokoch *et al*., 1998), which has been shown to phosphorylate RhoGDI and initiate Rac release (Dermardirossian *et al*., 2004). Our results provide evidence that DGKζ-derived PA activates PAK1, initiating the release of Rac1 from RhoGDI. This conclusion is supported by our findings that in DGKζ-null cells both active Rac1 and pPAK1 were substantially reduced, RhoGDI phosphorylation was decreased, and Rac release from RhoGDI was impaired. That Rac activation in the null cells was rescued by wt DGKζ, but not by a kinase inactive mutant, suggests enzymatic conversion of DAG to PA is required. Finally, addition of exogenous PA, but not DAG or LPA, increased Rac1 activity in the DGKζ-null MEFs.

PA may play multiple roles in Rac activation. In addition to stimulating PAK activity, negatively charged PA may function as a lipid anchor by binding positively charged residues at the C terminus of Rac1. Indeed, the polybasic region is required in addition to the C-terminal isoprenyl

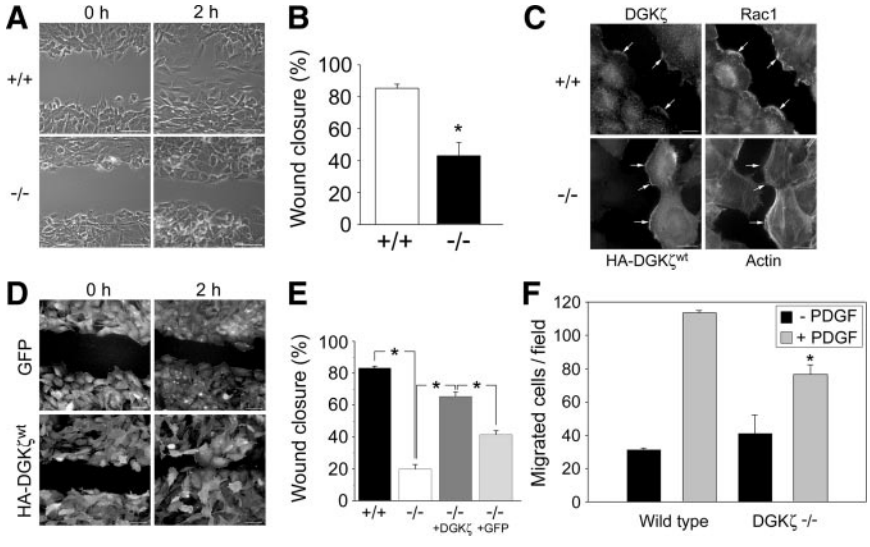

Figure 6. Reduced migration of DGKζ-null fibroblasts. (A) Phase-contrast images of wounded wt (+/+) and DGKζ-null (−/−) fibroblast monolayers taken immediately after wounding (0 h) or 2 h later. Bars, 50 μm. (B) Quantification of the wounding results in A. The graph shows the percent wound closure 2 h after wounding. Values are the mean ± SEM of four independent experiments. The asterisk denotes a significant difference from wt cells ($p < 0.005$) by Student's *t* test. (C) DGKζ is concentrated at the border of cells facing the wound. The wt fibroblasts were fixed and immunolabeled for endogenous DGKζ and Rac1 2 h after wounding. Null fibroblasts infected with adenovirus bearing HA-tagged DGKζ were fixed 2 h after wounding and stained with an anti-HA antibody and AlexaFluor 488-conjugated phalloidin to visualize actin. Arrows indicate protein concentrated at the leading edge of cells migrating into the wound. Bars, 20 μm. (D) Rescue of the migration defect by DGKζ overexpression. DGKζ-null cells were infected with adenovirus bearing either GFP or HA-tagged DGKζ and fixed at the indicated times after wounding. Cells were fixed and stained with anti-GFP (top) or anti-HA (bottom). Bar, 50 μm. (E) Quantification of percent wound closure at 2 h after wounding. Values are the mean ± SEM of at least 50 independent measurements per condition. An asterisk indicates a statistically significant difference ($p < 0.005$) by Student's *t* test. (F) Reduced three-dimensional migration of DGKζ-null fibroblasts. The wt and null fibroblasts were placed in the upper chamber of a Transwell migration plate and allowed to migrate across a porous membrane for 4 h in the absence (black bars) or presence (gray bars) of 10 ng/ml PDGF. The graph shows the mean number (± SEM) of migrated cells per field from two independent experiments. The asterisk indicates a significant difference from wt ($p < 0.05$).

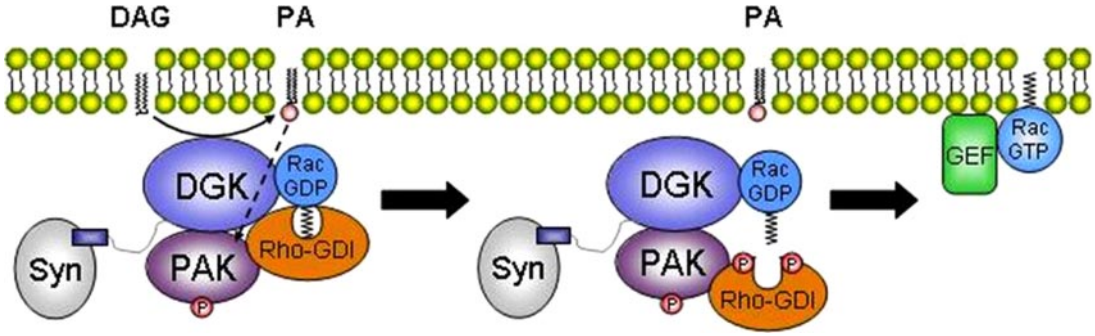

Figure 7. Model for the release of Rac1 from RhoGDI. Left, DGKζ-catalyzed conversion of DAG to PA (curved arrow) activates PAK1 (dashed arrow) which undergoes autophosphorylation (P). The C-terminal lipid moiety of Rac1-GDP is sequestered in a hydrophobic pocket of RhoGDI. Middle, PAK1-mediated phosphorylation of RhoGDI at two sites releases the lipid group. DGKζ binding to Rac1 may facilitate insertion of the lipid group into the plasma membrane. Right, membrane translocation allows Rac to interact with a GEF and to become activated. Syn, syntrophin.

group of Rac1 for membrane targeting (Joseph *et al*., 1994; Kreck *et al*., 1996; Ueyama *et al*., 2005). The interaction of the polybasic region with DGKζ-derived PA could facilitate shuttling of the C-terminal isoprenyl group from the hydrophobic pocket in RhoGDI to the inner leaflet of the plasma membrane.

Regulation of PAK Activity and Localization

The absence of DGKζ affected both the level and targeting of pPAK, without affecting total PAK1. However, pPAK levels were not reduced to zero, suggesting other phosphorylation mechanisms remain active in DGKζ-null cells. Both PDK1 and Akt phosphorylate PAK1 in response to PDGF stimulation (Franke *et al*., 1995; King *et al*., 2000; Tang *et al*., 2000), and Cdc42 can activate PAK upon adhesion to FN (Price *et al*., 1998). Because Akt and Cdc42 activities were largely unaffected in the DGKζ-null MEFs, they could account for the residual PAK phosphorylation.

In addition to phosphorylation, subcellular localization probably plays a key role in the regulation of PAK1 activity. In resting cells PAK1 localizes to cytosolic vesicles, but in stimulated cells, the active form accumulates in membrane ruffles and focal adhesions (Dharmawardhane *et al*., 1997; Manser *et al*., 1997; Sells *et al*., 2000). Targeting of active PAK to these structures influences cytoskeletal dynamics through phosphorylation of a variety of downstream effectors (Edwards *et al*., 1999; Sanders *et al*., 1999; Slack-Davis *et al*., 2003). The spatial regulation of PAK1 involves a GIT1-PIX-paxillin complex that promotes autophosphorylation and recruits the kinase from the cytosol to focal adhesions and the leading edge (Zhao *et al*., 2000; Manabe *et al*., 2002; Brown *et al*., 2002; Loo *et al*., 2004). Our data suggest DGKζ is also necessary for the translocation of pPAK1 from the cytosol to focal adhesions. In contrast, targeting of pPAK1 to membrane ruffles at the leading edge of the null cells was seemingly unaffected, so DGKζ does not seem to be required for this translocation event.

Integrin-mediated Cell Spreading

Integrins transduce signals from the extracellular matrix (ECM) to the actin cytoskeleton through pathways regulated by Rho GTPases (Clark *et al*., 1998). Focal adhesions serve as convergence points for rapid integration of growth factor- and integrin-mediated signaling responses (Plopper *et al*., 1995). Consistent with this idea, integrin engagement stimulates rapid assembly of structural and signaling components into focal adhesions, including both synthetic and degradative enzymes of the inositol lipid signaling cascade. Moreover, adhesion of fibroblasts to the ECM is required for PDGF-dependent hydrolysis of phosphatidylinositol bisphosphate (PIP_2) into DAG and inositol-1,4,5-trisphosphate (McNamee *et al*., 1993). Consistent with a defect in integrin-mediated signaling events, DGKζ-null MEFs exhibited reduced spreading after plating on FN. However, after longer periods, the surface area of DGKζ-null cells was not significantly different from wt cells. Because both lamellipodia and membrane ruffling were substantially decreased in the null cells, the residual spreading may be mediated by blunt filopodia and/or pseudopodia, which have been suggested to mediate spreading of Rac1-null cells (Vidali *et al*., 2006).

Integrins contribute to spatial regulation of Rac function by dissociating it from RhoGDI and enhancing its interaction with effectors at cell edges (Del Pozo *et al*., 2002). They also stimulate Rac membrane translocation by modulating the local lipid environment and preventing internalization of cholesterol-rich membrane domains (Del Pozo *et al*., 2004). Integrin activation stimulates PIP_2 hydrolysis to DAG by activating PLCγ (Auer and Jacobson, 1995); the latter reaction is enhanced by PDGF stimulation (McNamee *et al*., 1993). In this regard, DGKζ is positioned to integrate signals from the two inputs and to generate an output (PA) that activates PAK1 and dissociates Rac1 from RhoGDI.

Proposed Mechanism of Rac Release from RhoGDI

On the basis of these and previous findings (Tolias *et al*., 1998; Dermardirossian *et al*., 2004), we propose DGKζ exists in a multiprotein signaling complex with syntrophin, Rac1, PAK1 and RhoGDI and that DGKζ-derived PA activates PAK1, which subsequently phosphorylates RhoGDI to trigger Rac1 release (Figure 7). Thus, DGKζ occupies a key position in the signaling pathway from PIP_2 breakdown to Rac activation. Together, these results establish a mechanism whereby changes in lipid second messengers modulate the amount of active Rac and thus contribute to the regulation of the actin cytoskeleton.

ACKNOWLEDGMENTS

We thank Drs. Jonathan Chernoff and Jeffrey Peterson (Fox Chase Caner Center) for providing antibodies to pPAK1 and the PAK1 inhibitor, respectively. We thank Dr. Kaoru Goto for antibody to DGKι. The PAK1 GST-PBD construct was a gift from Dr. John Collard (The Netherlands Cancer Institute, Amsterdam, The Netherlands). We are grateful to Radoslav Zinoviev and

James Cheng for technical assistance. This work was supported by the Muscular Dystrophy Association USA and by the Cancer Research Society.

REFERENCES

Abercrombie, M., Heaysman, J. E., and Pegrum, S. M. (1970). The locomotion of fibroblasts in culture. I. Movements of the leading edge. Exp. Cell Res. *59*, 393–398.

Abramovici, H., and Gee, S, H. (2007). Morphological changes and spatial regulation of diacylglycerol kinase-zeta, syntrophins, and Rac1 during myoblast fusion. Cell Motil. Cytoskeleton *64*, 549–567.

Abramovici, H., Hogan, A. B., Obagi, C., Topham, M. K., and Gee, S. H. (2003). Diacylglycerol kinase-ζ localization in skeletal muscle is regulated by phosphorylation and interaction with syntrophins. Mol. Biol. Cell *14*, 4499–4511.

Auer, K. L., and Jacobson, B. S. (1995). Beta 1 integrins signal lipid second messengers required during cell adhesion. Mol. Biol. Cell *6*, 1305–1313.

Bagrodia, S., Bailey, D., Lenard, Z., Hart, M., Guan, J. L., Premont, R. T., Taylor, S. J., and Cerione, R. A. (1999). A tyrosine-phosphorylated protein that binds to an important regulatory region on the cool family of p21-activated kinase-binding proteins. J. Biol. Chem. *274*, 22393–22400.

Bokoch, G. M. (2003). Biology of the p21-activated kinases. Annu. Rev. Biochem. *72*, 743–781.

Bokoch, G. M., Reilly, A. M., Daniels, R. H., King, C. C., Olivera, A., Spiegel, S., and Knaus, U. G. (1998). A GTPase-independent mechanism of p21-activated kinase activation. Regulation by sphingosine and other biologically active lipids. J. Biol. Chem. *273*, 8137–8144.

Bokoch, G. M., Wang, Y., Bohl, B. P., Sells, M. A., Quilliam, L. A., and Knaus, U. G. (1996). Interaction of the Nck adapter protein with p21-activated kinase (PAK1). J. Biol. Chem. *271*, 25746–25749.

Bourmeyster, N., Stasia, M. J., Garin, J., Gagnon, J., Boquet, P., and Vignais, P. V. (1992). Copurification of rho protein and the rho-GDP dissociation inhibitor from bovine neutrophil cytosol. Effect of phosphoinositides on rho ADP-ribosylation by the C3 exoenzyme of *Clostridium botulinum*. Biochemistry *31*, 12863–12869.

Brown, M. C., West, K. A., and Turner, C. E. (2002). Paxillin-dependent paxillin kinase linker and p21-activated kinase localization to focal adhesions involves a multistep activation pathway. Mol. Biol. Cell *13*, 1550–1565.

Buccione, R., Orth, J. D., and McNiven, M. A. (2004). Foot and mouth: podosomes, invadopodia and circular dorsal ruffles. Nat. Rev. Mol. Cell Biol. *5*, 647–657.

Burridge, K., and Wennerberg, K. (2004). Rho and Rac take center stage. Cell *116*, 167–179.

Chuang, T. H., Bohl, B. P., and Bokoch, G. M. (1993a). Biologically active lipids are regulators of Rac.GDI complexation. J. Biol. Chem. *268*, 26206–26211.

Chuang, T. H., Xu, X., Knaus, U. G., Hart, M. J., and Bokoch, G. M. (1993b). GDP dissociation inhibitor prevents intrinsic and GTPase activating protein-stimulated GTP hydrolysis by the Rac GTP-binding protein. J. Biol. Chem. *268*, 775–778.

Clark, E. A., King, W. G., Brugge, J. S., Symons, M., and Hynes, R. O. (1998). Integrin-mediated signals regulated by members of the rho family of GTPases. J. Cell Biol. *142*, 573–586.

Deacon, S. W., Beeser, A., Fukui, J. A., Rennefahrt, U. E., Myers, C., Chernoff, J., and Peterson, J. R. (2008). An isoform-selective, small-molecule inhibitor targets the autoregulatory mechanism of p21-activated kinase. Chem. Biol. *15*, 322–331.

Del Pozo, M. A., Alderson, N. B., Kiosses, W. B., Chiang, H. H., Anderson, G. G., and Schwartz, M. A. (2004). Integrins regulate Rac targeting by internalization of membrane domains. Science *303*, 839–842.

Del Pozo, M. A., Kiosses, W. B., Alderson, N. B., Meller, N., Hahn, K. M., and Schwartz, M. A. (2002). Integrins regulate GTP-Rac localized effector interactions through dissociation of Rho-GDI. Nat. Cell Biol. *4*, 232–239.

Dermardirossian, C., and Bokoch, G. M. (2005). GDIs: central regulatory molecules in Rho GTPase activation. Trends Cell Biol. *15*, 356–363.

Dermardirossian, C., Schnelzer, A., and Bokoch, G. M. (2004). Phosphorylation of RhoGDI by Pak1 mediates dissociation of Rac GTPase. Mol. Cell *15*, 117–127.

Dharmawardhane, S., Sanders, L. C., Martin, S. S., Daniels, R. H., and Bokoch, G. M. (1997). Localization of p21-activated kinase 1 (PAK1) to pinocytic vesicles and cortical actin structures in stimulated cells. J. Cell Biol. *138*, 1265–1278.

Dovas, A., and Couchman, J. R. (2005). RhoGDI: multiple functions in the regulation of Rho family GTPase activities. Biochem. J. *390*, 1–9.

Edwards, D. C., Sanders, L. C., Bokoch, G. M., and Gill, G. N. (1999). Activation of LIM-kinase by Pak1 couples Rac/Cdc42 GTPase signalling to actin cytoskeletal dynamics. Nat. Cell Biol. *1*, 253–259.

Faure, J., Vignais, P. V., and Dagher, M. C. (1999). Phosphoinositide-dependent activation of Rho A involves partial opening of the RhoA/Rho-GDI complex. Eur. J. Biochem. *262*, 879–889.

Fenteany, G., Janmey, P. A., and Stossel, T. P. (2000). Signaling pathways and cell mechanics involved in wound closure by epithelial cell sheets. Curr. Biol. *10*, 831–838.

Franke, T. F., Yang, S. I., Chan, T. O., Datta, K., Kazlauskas, A., Morrison, D. K., Kaplan, D. R., and Tsichlis, P. N. (1995). The protein kinase encoded by the Akt proto-oncogene is a target of the PDGF-activated phosphatidylinositol 3-kinase. Cell *81*, 727–736.

Guo, F., Debidda, M., Yang, L., Williams, D. A., and Zheng, Y. (2006). Genetic deletion of Rac1 GTPase reveals its critical role in actin stress fiber formation and focal adhesion complex assembly. J. Biol. Chem. *281*, 18652–18659.

Hogan, A., Shepherd, L., Chabot, J., Quenneville, S., Prescott, S. M., Topham, M. K., and Gee, S. H. (2001). Interaction of gamma 1-syntrophin with diacylglycerol kinase-zeta. Regulation of nuclear localization by PDZ interactions. J. Biol. Chem. *276*, 26526–26533.

Jaffe, A. B., and Hall, A. (2005). RHO GTPASES: biochemistry and biology. Annu. Rev. Cell Dev. Biol. *21*, 247–269.

Joseph, G., Gorzalczany, Y., Koshkin, V., and Pick, E. (1994). Inhibition of NADPH oxidase activation by synthetic peptides mapping within the carboxyl-terminal domain of small GTP-binding proteins. Lack of amino acid sequence specificity and importance of polybasic motif. J. Biol. Chem. *269*, 29024–29031.

King, C. C., Zenke, F. T., Dawson, P. E., Dutil, E. M., Newton, A. C., Hemmings, B. A., and Bokoch, G. M. (2000). Sphingosine is a novel activator of 3-phosphoinositide-dependent kinase 1. J. Biol. Chem. *275*, 18108–18113.

Kreck, M. L., Freeman, J. L., Abo, A., and Lambeth, J. D. (1996). Membrane association of Rac is required for high activity of the respiratory burst oxidase. Biochemistry *35*, 15683–15692.

Loo, T. H., Ng, Y. W., Lim, L., and Manser, E. (2004). GIT1 activates p21-activated kinase through a mechanism independent of p21 binding. Mol. Cell. Biol. *24*, 3849–3859.

Luo, B., Prescott, S. M., and Topham, M. K. (2004a). Diacylglycerol kinase zeta regulates phosphatidylinositol 4-phosphate 5-kinase Ialpha by a novel mechanism. Cell Signal. *16*, 891–897.

Luo, B., Regier, D. S., Prescott, S. M., and Topham, M. K. (2004b). Diacylglycerol kinases. Cell Signal. *16*, 983–989.

Manabe, R., Kovalenko, M., Webb, D. J., and Horwitz, A. R. (2002). GIT1 functions in a motile, multi-molecular signaling complex that regulates protrusive activity and cell migration. J. Cell Sci. *115*, 1497–1510.

Manser, E., Huang, H. Y., Loo, T. H., Chen, X. Q., Dong, J. M., Leung, T., and Lim, L. (1997). Expression of constitutively active alpha-PAK reveals effects of the kinase on actin and focal complexes. Mol. Cell. Biol. *17*, 1129–1143.

Manser, E., Loo, T. H., Koh, C. G., Zhao, Z. S., Chen, X. Q., Tan, L., Tan, I., Leung, T., and Lim, L. (1998). PAK kinases are directly coupled to the PIX family of nucleotide exchange factors. Mol. Cell *1*, 183–192.

McNamee, H. P., Ingber, D. E., and Schwartz, M. A. (1993). Adhesion to fibronectin stimulates inositol lipid synthesis and enhances PDGF-induced inositol lipid breakdown. J. Cell Biol. *121*, 673–678.

Mehta, D., Rahman, A., and Malik, A. B. (2001). Protein kinase C-alpha signals rho-guanine nucleotide dissociation inhibitor phosphorylation and rho activation and regulates the endothelial cell barrier function. J. Biol. Chem. *276*, 22614–22620.

Menard, R. E., and Mattingly, R. R. (2003). Cell surface receptors activate p21-activated kinase 1 via multiple Ras and PI3-kinase-dependent pathways. Cell Signal. *15*, 1099–1109.

Mesmin, B., Robbe, K., Geny, B., Luton, F., Brandolin, G., Popoff, M. R., and Antonny, B. (2004). A phosphatidylserine-binding site in the cytosolic fragment of *Clostridium sordellii* lethal toxin facilitates glucosylation of membrane-bound Rac and is required for cytotoxicity. J. Biol. Chem. *279*, 49876–49882.

Nobes, C. D., and Hall, A. (1995). Rho, rac, and cdc42 GTPases regulate the assembly of multimolecular focal complexes associated with actin stress fibers, lamellipodia, and filopodia. Cell *81*, 53–62.

Nobes, C. D., and Hall, A. (1999). Rho GTPases control polarity, protrusion, and adhesion during cell movement. J. Cell Biol. *144*, 1235–1244.

Olofsson, B. (1999). Rho guanine dissociation inhibitors: pivotal molecules in cellular signalling. Cell Signal. *11*, 545–554.

Plopper, G. E., McNamee, H. P., Dike, L. E., Bojanowski, K., and Ingber, D. E. (1995). Convergence of integrin and growth factor receptor signaling pathways within the focal adhesion complex. Mol. Biol. Cell *6*, 1349–1365.

Price, L. S., Leng, J., Schwartz, M. A., and Bokoch, G. M. (1998). Activation of Rac and Cdc42 by integrins mediates cell spreading. Mol. Biol. Cell *9*, 1863–1871.

Ren, X. D., Kiosses, W. B., and Schwartz, M. A. (1999). Regulation of the small GTP-binding protein Rho by cell adhesion and the cytoskeleton. EMBO J. *18*, 578–585.

Ridley, A. J. (2006). Rho GTPases and actin dynamics in membrane protrusions and vesicle trafficking. Trends Cell Biol. *16*, 522–529.

Ridley, A. J., Paterson, H. F., Johnston, C. L., Diekmann, D., and Hall, A. (1992). The small GTP-binding protein rac regulates growth factor-induced membrane ruffling. Cell *70*, 401–410.

Robertson, E. J. (1987). Embryo derived stem cell lines. In: Teratocarcinomas and Embryonic Stem Cells: A Practical Approach, ed. E. J. Robertson. Oxford, NY: IRL Press, 71–112.

Sander, E. E., van Delft, S., ten Klooster, J. P., Reid, T., van der Kammen, R. A., Michiels, F., and Collard, J. G. (1998). Matrix-dependent Tiam1/Rac signaling in epithelial cells promotes either cell-cell adhesion or cell migration and is regulated by phosphatidylinositol 3-kinase. J. Cell Biol. *143*, 1385–1398.

Sanders, L. C., Matsumura, F., Bokoch, G. M., and de Lanerolle, P. (1999). Inhibition of myosin light chain kinase by p21-activated kinase. Science *283*, 2083–2085.

Sells, M. A., Knaus, U. G., Bagrodia, S., Ambrose, D. M., Bokoch, G. M., and Chernoff, J. (1997). Human p21-activated kinase (Pak1) regulates actin organization in mammalian cells. Curr. Biol. *7*, 202–210.

Sells, M. A., Pfaff, A., and Chernoff, J. (2000). Temporal and spatial distribution of activated Pak1 in fibroblasts. J. Cell Biol. *151*, 1449–1458.

Slack-Davis, J. K., Eblen, S. T., Zecevic, M., Boerner, S. A., Tarcsafalvi, A., Diaz, H. B., Marshall, M. S., Weber, M. J., Parsons, J. T., and Catling, A. D. (2003). PAK1 phosphorylation of MEK1 regulates fibronectin-stimulated MAPK activation. J. Cell Biol. *162*, 281–291.

Takahashi, Y., Nakayama, T., Soma, M., Izumi, Y., and Kanmatsuse, K. (1997). CA repeat polymorphism of the neuronal nitric oxide synthase gene. Hum. Hered. *47*, 58–59.

Tang, Y., Zhou, H., Chen, A., Pittman, R. N., and Field, J. (2000). The Akt proto-oncogene links Ras to Pak and cell survival signals. J. Biol. Chem. *275*, 9106–9109.

Tolias, K. F., Couvillon, A. D., Cantley, L. C., and Carpenter, C. L. (1998). Characterization of a Rac1- and RhoGDI-associated lipid kinase signaling complex. Mol. Cell. Biol. *18*, 762–770.

Tolias, K. F., Hartwig, J. H., Ishihara, H., Shibasaki, Y., Cantley, L. C., and Carpenter, C. L. (2000). Type Ialpha phosphatidylinositol-4-phosphate 5-kinase mediates Rac-dependent actin assembly. Curr. Biol. *10*, 153–156.

Topham, M. K., Bunting, M., Zimmerman, G. A., McIntyre, T. M., Blackshear, P. J., and Prescott, S. M. (1998). Protein kinase C regulates the nuclear localization of diacylglycerol kinase-zeta. Nature *394*, 697–700.

Topham, M. K., and Prescott, S. M. (2001). Diacylglycerol kinase zeta regulates Ras activation by a novel mechanism. J. Cell Biol. *152*, 1135–1143.

Ueyama, T., Eto, M., Kami, K., Tatsuno, T., Kobayashi, T., Shirai, Y., Lennartz, M. R., Takeya, R., Sumimoto, H., and Saito, N. (2005). Isoform-specific membrane targeting mechanism of Rac during Fc gamma R-mediated phagocytosis: positive charge-dependent and independent targeting mechanism of Rac to the phagosome. J. Immunol. *175*, 2381–2390.

Ugolev, Y., Molshanski-Mor, S., Weinbaum, C., and Pick, E. (2006). Liposomes comprising anionic but not neutral phospholipids cause dissociation of Rac(1 or 2) x RhoGDI complexes and support amphiphile-independent NADPH oxidase activation by such complexes. J. Biol. Chem. *281*, 19204–19219.

Vidali, L., Chen, F., Cicchetti, G., Ohta, Y., and Kwiatkowski, D. J. (2006). Rac1-null mouse embryonic fibroblasts are motile and respond to platelet-derived growth factor. Mol. Biol. Cell *17*, 2377–2390.

Wagner, S., Flood, T. A., O'Reilly, P., Hume, K., and Sabourin, L. A. (2002). Association of the Ste20-like kinase (SLK) with the microtubule. Role in Rac1-mediated regulation of actin dynamics during cell adhesion and spreading. J. Biol. Chem. *277*, 37685–37692.

Welch, H., Eguinoa, A., Stephens, L. R., and Hawkins, P. T. (1998). Protein kinase B and rac are activated in parallel within a phosphatidylinositide 3OH-kinase-controlled signaling pathway. J. Biol. Chem. *273*, 11248–11256.

Yakubchyk, Y., Abramovici, H., Maillet, J. C., Daher, E., Obagi, C., Parks, R. J., Topham, M. K., and Gee, S. H. (2005). Regulation of neurite outgrowth in N1E-115 cells through PDZ-mediated recruitment of diacylglycerol kinase {zeta}. Mol. Cell. Biol. *25*, 7289–7302.

Yamashita, T., and Tohyama, M. (2003). The p75 receptor acts as a displacement factor that releases Rho from Rho-GDI. Nat. Neurosci. *6*, 461–467.

Zhao, Z. S., Manser, E., Loo, T. H., and Lim, L. (2000). Coupling of PAK-interacting exchange factor PIX to GIT1 promotes focal complex disassembly. Mol. Cell. Biol. *20*, 6354–6363.

Zhong, X. P., Hainey, E. A., Olenchock, B. A., Jordan, M. S., Maltzman, J. S., Nichols, K. E., Shen, H., and Koretzky, G. A. (2003). Enhanced T cell responses due to diacylglycerol kinase zeta deficiency. Nat. Immunol. *4*, 882–890.